Supplementary Information for

Selective Etching of Binary Nanoparticle Superlattices via Thermally-induced Asymmetric Ligand Evolution

*Di Lei,[a] Hao Wang,[a] Ting Wang,[a] Fangyue Wu,[a] Ning Ding,[a] Yajun Wang[*b], Tongtao Li,[*a] and Angang Dong[*a]*

[a]*Shanghai Key Laboratory of Molecular Catalysis and Innovative Materials and Department of Chemistry, Fudan University, Shanghai 200433, China. ttli@fudan.edu.cn; agdong@fudan.edu.cn*

[b]*College of Chemistry and Materials Engineering, Wenzhou University, Wenzhou 325027, China. E-mail: yajunwang@wzu.edu.cn*

Experimental Section

Materials

Rare earth (RE = Y, Yb, Er, Gd, Nd) chlorate hydrates ($RECl_3 \cdot 6H_2O$, 99.9%), iron(III) chloride hexahydrate ($FeCl_3 \cdot 6H_2O$, 97%), 1-octadecene (ODE, 90%), and oleic acid (OA, 90%) were purchased from Sigma-Aldrich. Ammonium fluoride (NH_4F, >98%) was obtained from Alfa Aesar. Sodium hydroxide (NaOH, AR), potassium hydroxide (KOH, AR), oxalic acid dihydrate (>99.5%), methanol (AR), ethanol (AR), and n-hexane (AR) were purchased from Sinopharm Chemical Reagent Co., Ltd. All chemicals were used as received without further purification.

Synthesis of faceted β-$NaYF_4$:Yb/Er nanocrystals (NCs)

The faceted β-$NaYF_4$:Yb/Er NSs used here were synthesized following a literature method.[1] In a typical synthesis of β-$NaYF_4$:Yb/Er NCs, a rare earth chloride hexahydrate mixture consisting of 1 mmol $RECl_3 \cdot 6H_2O$ (comprising 80% Y, 18% Yb, and 2% Er) was combined with 6 mL of OA and 15 mL of ODE in a 50-mL three-neck flask. After degassing, the flask was then heated to 150 °C under a nitrogen atmosphere to yield a clear, homogeneous solution. Upon cooling to room temperature, the solution was treated with 6 mL of methanol containing NaOH (2.5 mmol) and NH_4F (4 mmol). The resultant mixture was gradually heated to 110 °C to ensure the complete evaporation of methanol, followed by a rapid temperature increase to 300 °C and maintenance at this temperature for 1 hour to facilitate NC formation. Upon cooling to room temperature, ethanol was introduced to precipitate the NCs. The precipitated NCs were subjected to a purification process involving washes with hexane and ethanol, performed at least once to ensure removal of impurities. The purified $NaYF_4$:Yb/Er NCs were re-dispersed in hexane for subsequent self-assembly experiments.

Synthesis of colloidal Fe_3O_4 NCs

Fe_3O_4 nanospheres (NSs) with tunable diameters were synthesized by the thermal decomposition of iron oleate.[2] Briefly, 9 g of iron oleate and 1.2 g of OA were dispersed in 45 mL of ODE, and the mixture was degassed at 120 ℃ under vacuum for 1 h. Then,

the solution was heated to 320 ℃ and kept for 1 h under inert atmosphere. The resulting Fe_3O_4 NSs, with OA as ligands, were dispersed in n-hexane for further use.

Synthesis of β-$NaYF_4$: Yb/Er@$NaGdF_4$@$NaNdF_4$ nanodumbbells (NDs)

β-$NaYF_4$:Yb/Er@$NaGdF_4$@$NaNdF_4$ nanodumbbells were synthesized via a modified literature method using a two-step epitaxial growth process.[1] In a 50 mL three-neck flask, $GdCl_3 \cdot 6H_2O$ (0.2 mmol) was dissolved in 3 mL of OA and 8 mL of ODE under stirring. The mixture was degassed under nitrogen and heated to 150 °C until a clear solution formed, then allowed to cool to room temperature. A methanol solution (10 mL) containing NaOH (2 mmol) and NH_4F (0.7 mmol) was then added, followed by the introduction of 30 nm β-$NaYF_4$: Yb/Er core NCs (0.2 mmol). The resulting mixture was slowly heated to 110 °C to evaporate methanol and subsequently raised to 310 °C, where it was maintained for 1 h to grow the $NaGdF_4$ shell. After cooling to room temperature, the NCs were precipitated by ethanol, washed at least twice with hexane and ethanol, and re-dispersed in 5 mL of toluene. In a separate 50 mL flask, $NdCl_3 \cdot 6H_2O$ (0.1 mmol) was mixed with 3 mL OA and 8 mL ODE. The mixture was degassed and heated to 150 °C until clear, then cooled to room temperature. A 6 mL methanol solution containing KOH (0.2 mmol), NaOH (0.2 mmol), and NH_4F (0.3 mmol) was added, followed by the introduction of the as synthesized β-$NaYF_4$: Yb/Er@$NaGdF_4$ NCs (0.1 mmol). The mixture was again heated to 110 °C to remove methanol, then rapidly raised to 310 °C and maintained for 30 min to grow the $NaNdF_4$ shell. The final β-$NaYF_4$: Yb/Er@$NaGdF_4$@$NaNdF_4$ nanodumbbells were purified by ethanol precipitation, washed with hexane and ethanol, and re-dispersed in 5 mL of hexane for storage and further use.

Self-assembly of BNSLs on the air-liquid surface

In a typical process, a 20 μL of n-hexane solution containing the as-formed NDs and NSs with proper concentration ratios was spread on the diethylene glycol (DEG) surface in a Teflon well. The well was covered with a glass slide to control the evaporation rate. A solid film formed on the DEG surface after the complete evaporation of hexane, which can then be transferred to TEM grids or Si wafers for subsequent characterization.

Thermal Treatment and Selective Etching of Binary Superlattices

The as-assembled superlattice films supported on carbon-coated copper TEM grids were subjected to a controlled thermal treatment prior to etching. The copper grids were placed in an open glass Petri dish on a heating stage, where the actual temperature was stabilized at 150 °C under infrared camera monitoring. The samples were then heated for a prescribed duration (0–8 h). After thermal treatment, the nanocrystal cores were selectively removed by chemical etching. The heated grids were immersed in 10 mL of 0.01 M aqueous oxalic acid solution and allowed to react at room temperature for 0–8 min, with the etching time precisely controlled. Depending on the prior thermal treatment time, the etching selectively removed either the $NaYF_4$ or the Fe_3O_4 component: at shorter heating times, $NaYF_4$ nanocrystals were preferentially etched, whereas extended heating rendered $NaYF_4$ acid-resistant and shifted the etching selectivity to Fe_3O_4. After etching, the grids were thoroughly rinsed with deionized water and dried under ambient conditions. In all cases, a non-close-packed ordered nanoparticle array was obtained, which preserves the registry and symmetry of the parent binary superlattice.

Materials characterization

Transmission electron microscopy (TEM) was carried out on a Hitachi HT 7700 microscope (120 kV). High-resolution TEM (HRTEM), high-angle annular dark-field scanning TEM (HAADF-STEM) images, elemental mapping and small-angle electron diffraction (SAED) were conducted on a Tecnai G2 F20 S-Twin microscope (200 kV). Scanning electron microscopy (SEM) images were recorded on a Zeiss Ultra55 microscope operated at 3 kV. Fourier transform infrared (FTIR) spectra were measured using a PerkinElmer Spectrum Two spectrometer. Nuclear magnetic resonance (NMR) spectra were acquired using a Bruker AVANCE III HD 400 MHz instrument. X-ray photoelectron spectroscopy (XPS) was performed on a Thermo Scientific K-Alpha instrument. For bulk analyses, single-component nanocrystal dispersions were drop-cast onto silicon substrates and thermally treated as needed. For ^1H NMR analysis, the treated nanocrystals were redispersed in deuterated solvent, while FTIR and XPS measurements were performed directly on the as-deposited nanocrystal films.

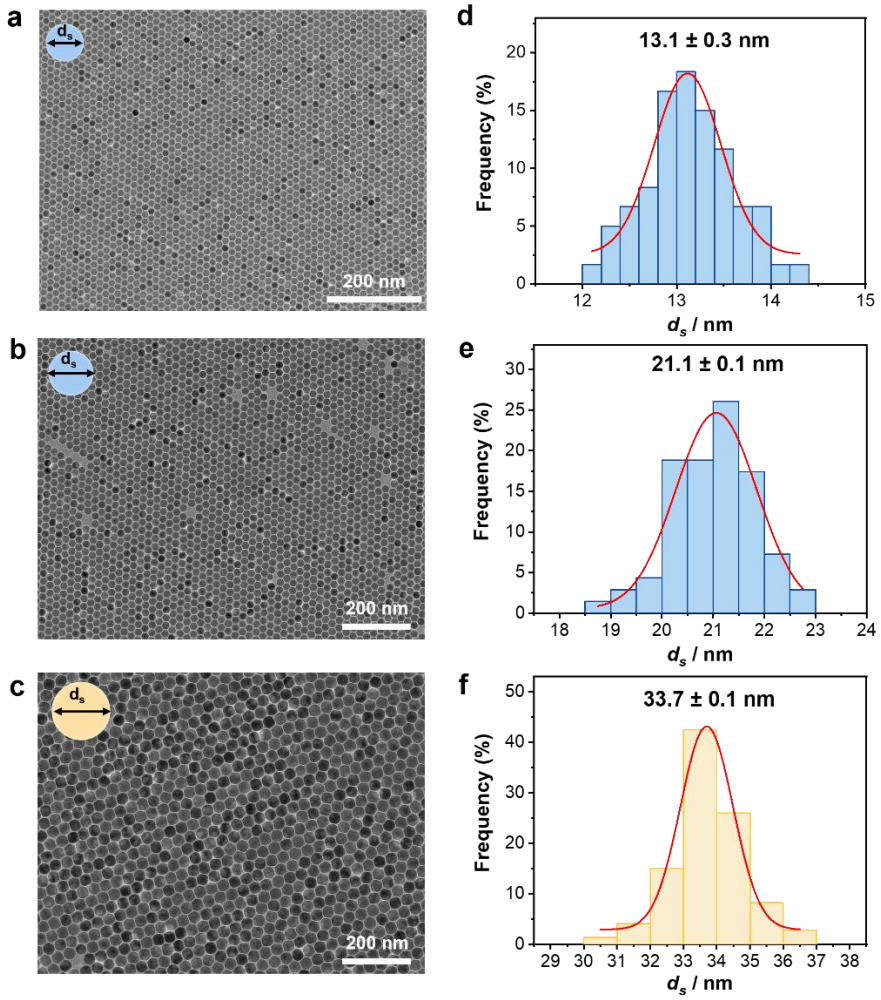

Figure S1. TEM images (left column) and corresponding size (d_s) distributions (right column) of Fe_3O_4 NSs with various diameters: (a) 13.1 nm; (b) 21.1 nm and (c) 33.7 nm.

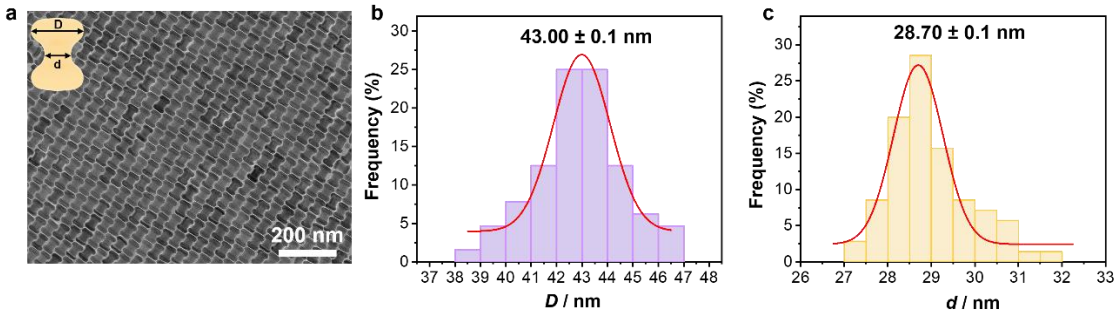

Figure S2. (a) TEM image of β-$NaYF_4$:Yb/Er@$NaGdF_4$@$NaNdF_4$ NDs with corresponding schematics (inset), and corresponding size distributions: (b) histograms of the *D* distribution, and (c) histograms of the *d* distribution for NDs. *D* represents the diagonal length of the hexagonal heads and *d* represents the narrowest diameter of the cylindrical waist.

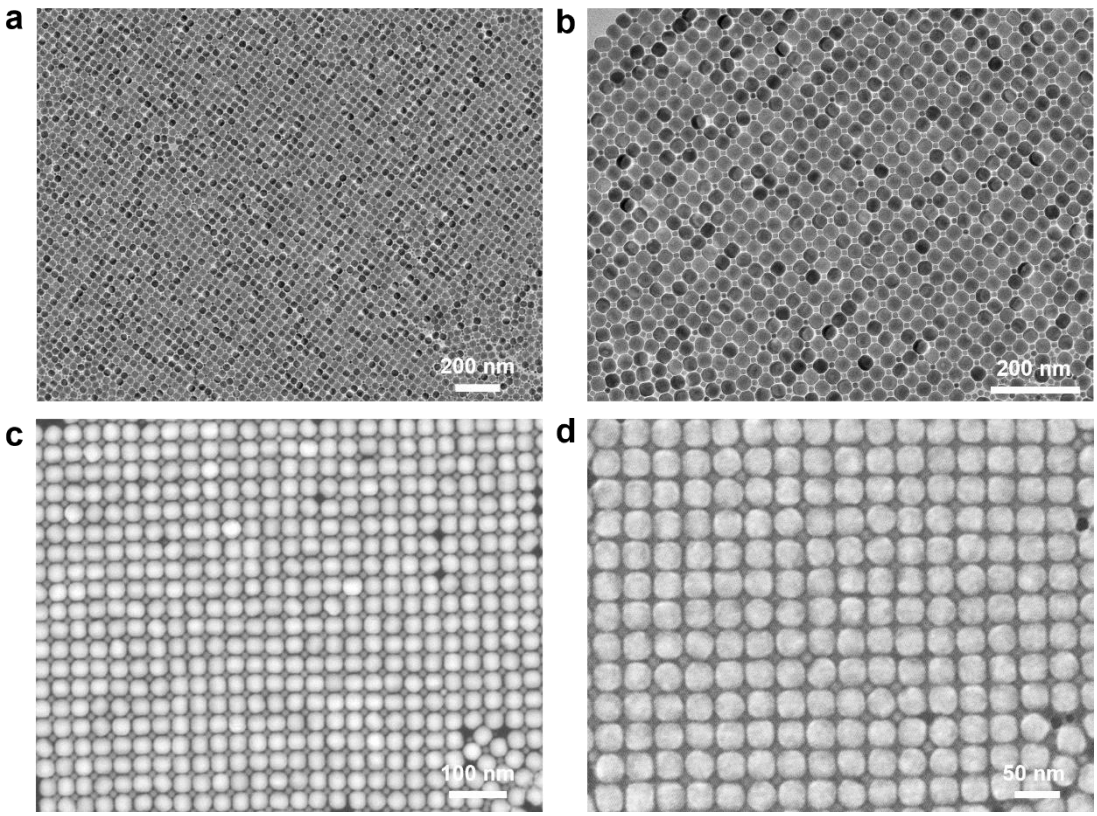

Figure S3. (a) Low- and (b) high-magnification TEM images of the AB-type BNSLs from the co-assembly of $NaYF_4$ and Fe_3O_4 NCs. (c) HAADF-STEM image, and (d) SEM image.

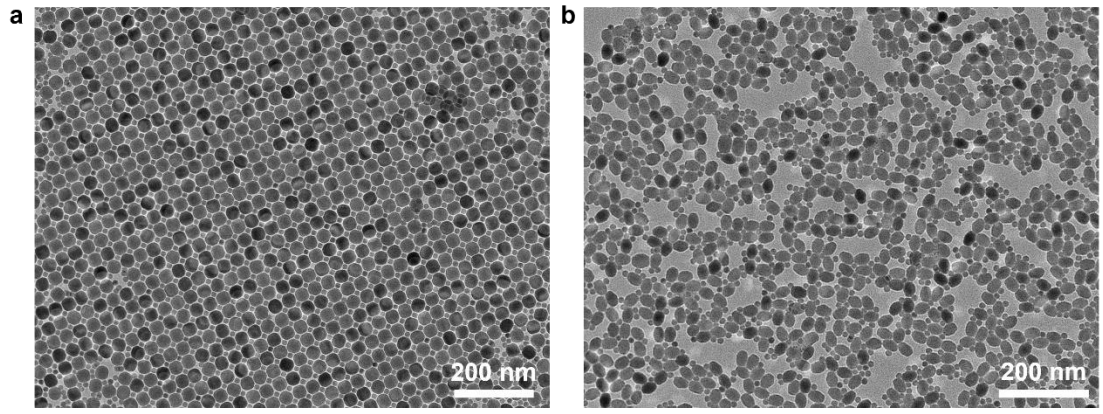

Figure S4. (a) TEM image of pristine AB-type BNSLs without thermal treatment. (b) TEM image of BNSLs directly etched in 0.01 M oxalic acid without prior heating. The ordered superstructure collapses during etching, while $NaYF_4$ NCs are preferentially removed.

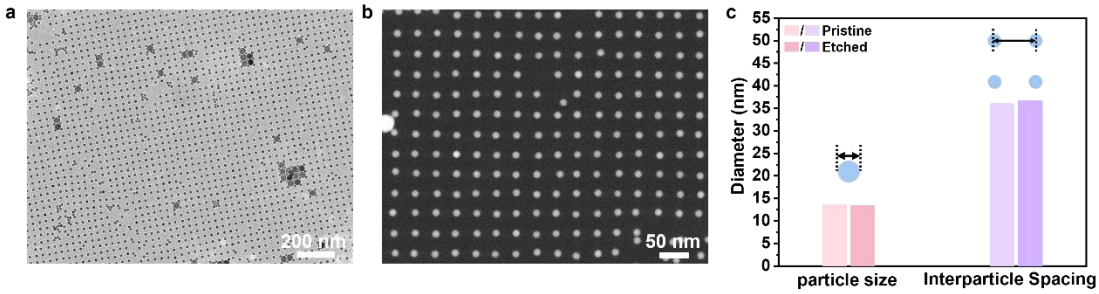

Figure S5. Characterization of the Fe_3O_4 nanoparticle arrays obtained after selective removal of $NaYF_4$ from AB-type BNSLs. (a) Low-magnification TEM image. (b) HAADF-STEM image. (c) Statistical analysis of Fe_3O_4 nanoparticle diameter and interparticle spacing before and after etched, confirming that the ordered registry is preserved while the $NaYF_4$ component is removed.

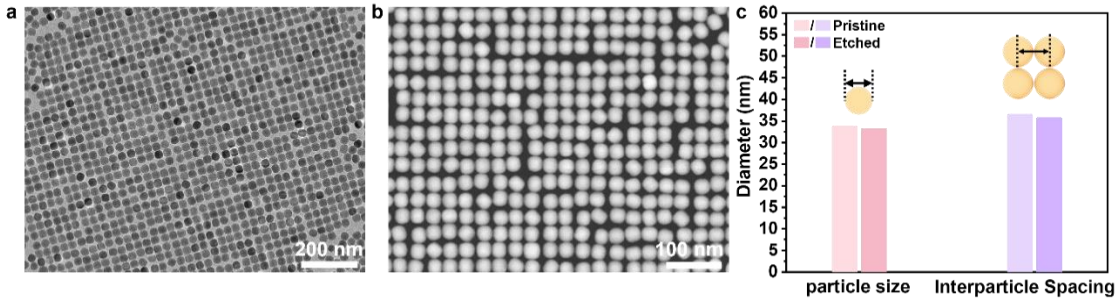

Figure S6. Characterization of the $NaYF_4$ nanoparticle arrays obtained after selective removal of Fe_3O_4 from AB-type BNSLs. (a) Low-magnification TEM image. (b) HAADF-STEM image. (c) Statistical analysis of $NaYF_4$ nanoparticle diameter and interparticle spacing before and after etched, confirming that the ordered registry is preserved while the Fe_3O_4 component is removed.

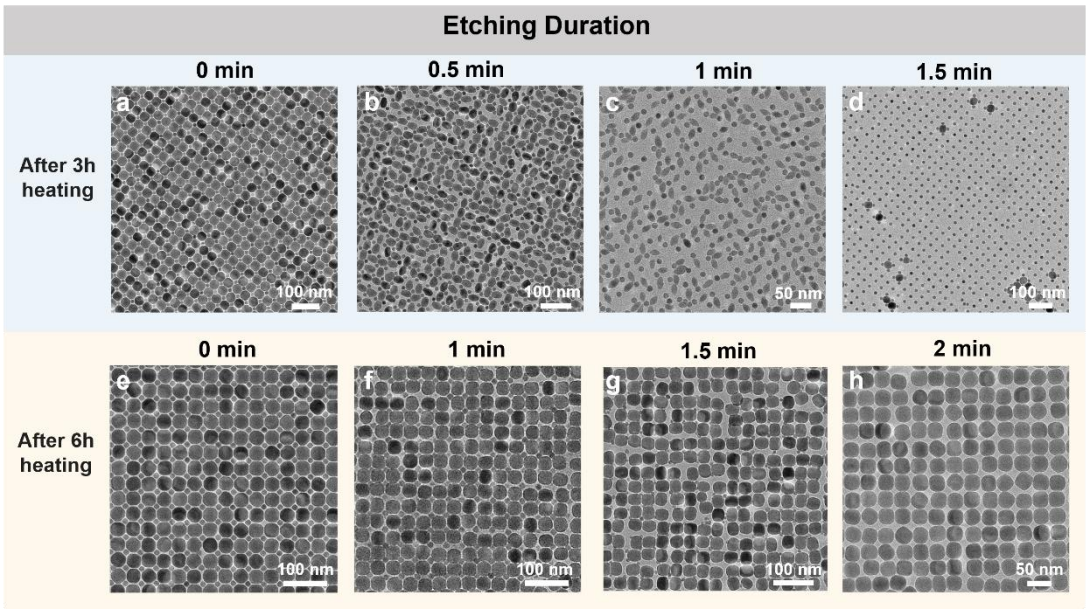

Figure S7. TEM images showing the duration-dependent, stepwise etching of AB-type BNSLs in 0.01 M oxalic acid. (a–d) Samples preheated at 150 °C for 3 h and etched for 0, 0.5, 1, and 1.5 min, respectively, demonstrating the preferential removal of $NaYF_4$ NCs while the ordered superlattice framework remains fixed. (e–h) Samples preheated at 150 °C for 6 h and etched for 0, 1, 1.5, and 2 min, respectively, showing the selective removal of Fe_3O_4 NCs with the lattice preserved. These images highlight the progressive nature of the etching process and the thermally controlled inversion of selectivity.

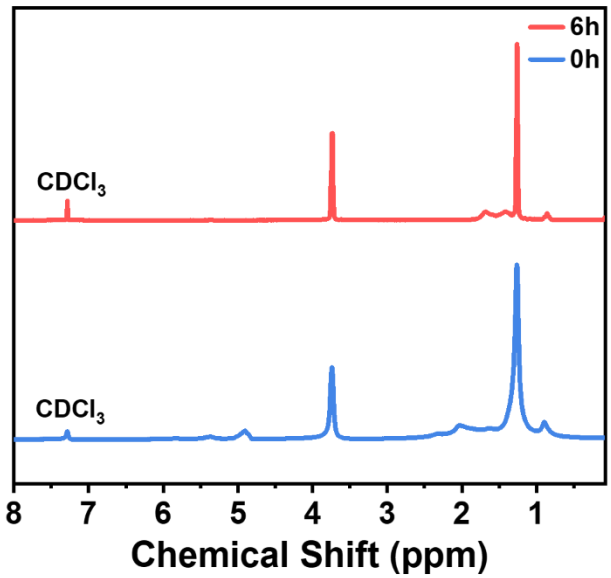

Figure S8. ^{1}H NMR spectrum of $NaYF_4$ NCs after thermal treatment for 0 h and 6 h.

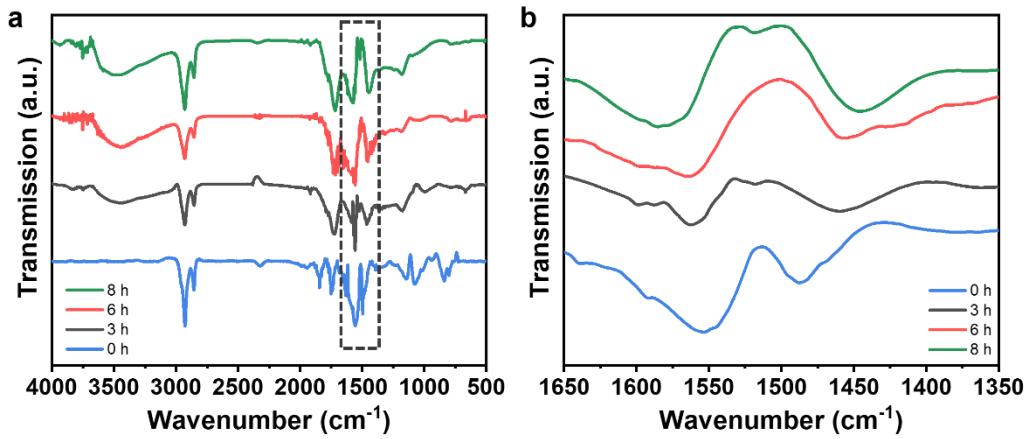

Figure S9. (a) FTIR spectra of $NaYF_4$ NCs after thermal treatment for 0, 3, 6, and 8 h. (b) Enlarged view of the 1650–1350 cm^{-1} region highlighting the asymmetric (ν_{as}) and symmetric (ν_s) stretching vibrations of the carboxylate groups from surface-bound oleate ligands. With increasing thermal treatment time, the band separation $\Delta\nu = \nu_{as} - \nu_s$ progressively increases from 65 to 95, 105 and 130 cm^{-1}, indicating a continuous evolution of the carboxylate coordination environment.[3]

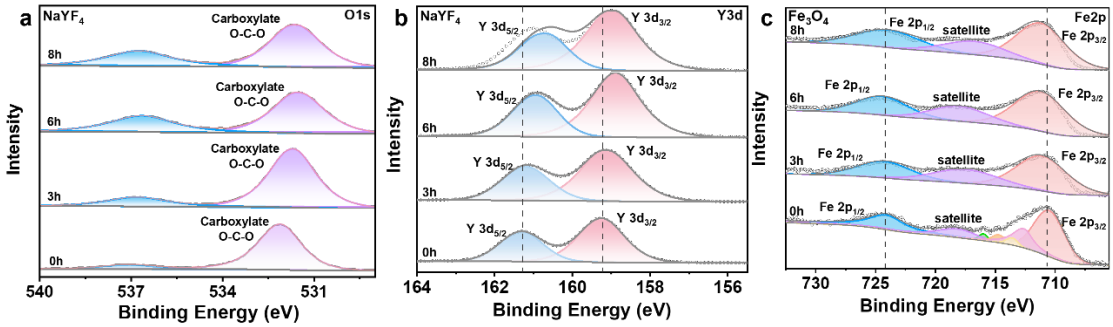

Figure S10. (a) O 1s and (b) Y 3d XPS spectra of $NaYF_4$ NCs obtained after thermal treatment for 0, 3, 6, and 8 h, respectively. (c) Fe 2p XPS spectra of Fe_3O_4 NCs obtained after thermal treatment for 0, 3, 6 and 8 h, respectively.

Complementary information is provided by the O 1s and Y 3d regions of $NaYF_4$. In the O 1s spectra, a weak high-binding-energy component at 536.6–536.8 eV becomes more evident with increasing heating time, reflecting changes in the chemical environment of oxygen species associated with surface carboxylates. Meanwhile, the Y 3d peaks shift slightly toward lower binding energies, indicating an increase in local electron density around surface Y^{3+} ions.[4] This behavior is consistent with deprotonation of carboxylic groups and stronger coordination of carboxylates to Y^{3+} centers, supporting the formation of a chemically reconstructed and densified ligand shell on $NaYF_4$ NCs.

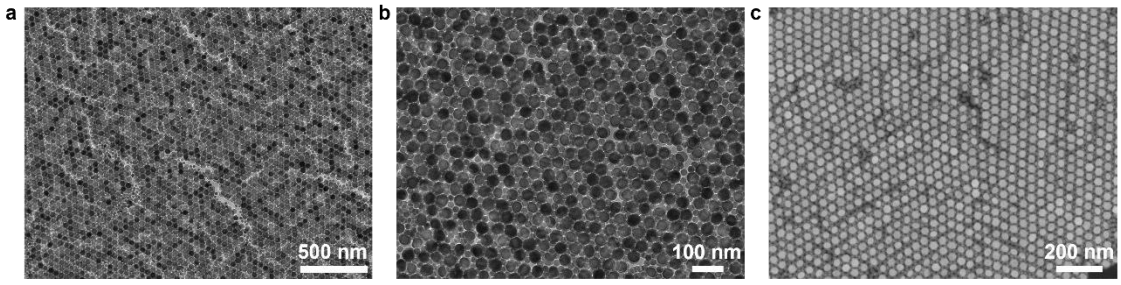

Figure S11. (a) Low- and (b) high-magnification TEM images of the AB_2-type BNSLs from the co-assembly of β-$NaYF_4$:Yb/Er@$NaGdF_4$@$NaNdF_4$ NDs and Fe_3O_4 NSs. (c) HAADF-STEM image.

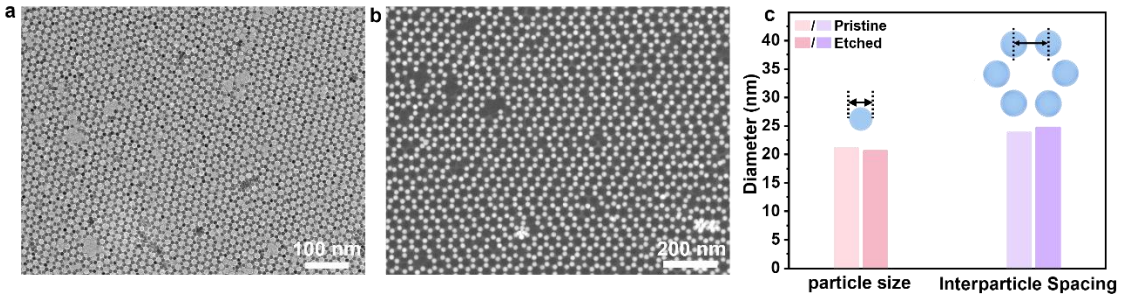

Figure S12. Characterization of the sphere NCs arrays obtained after selective removal of the nanodumbbells NCs from AB_2-type BNSLs. (a) Low-magnification TEM image. (b) HAADF-STEM image. (c) Statistical analysis of Fe_3O_4 nanoparticle diameter and interparticle spacing before and after etched, confirming that the ordered registry is preserved while NDs is removed.

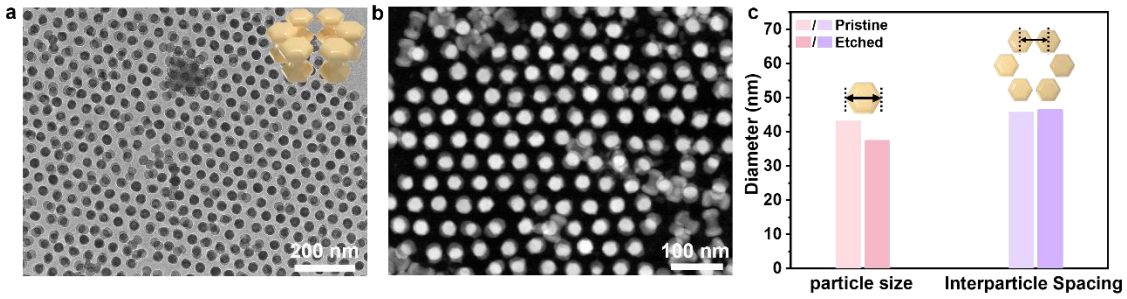

Figure S13. Characterization of the nanodumbbells NCs arrays obtained after selective removal of the sphere NCs from AB_2-type BNSLs. (a) Low-magnification TEM image (inset: side-view schematic of NDs arrays). (b) HAADF-STEM image. (d) Statistical analysis of the head size of the nanodumbbells NCs and the interparticle spacing before and after etched, confirming that the ordered registry is preserved while the Fe_3O_4 NSs is removed.

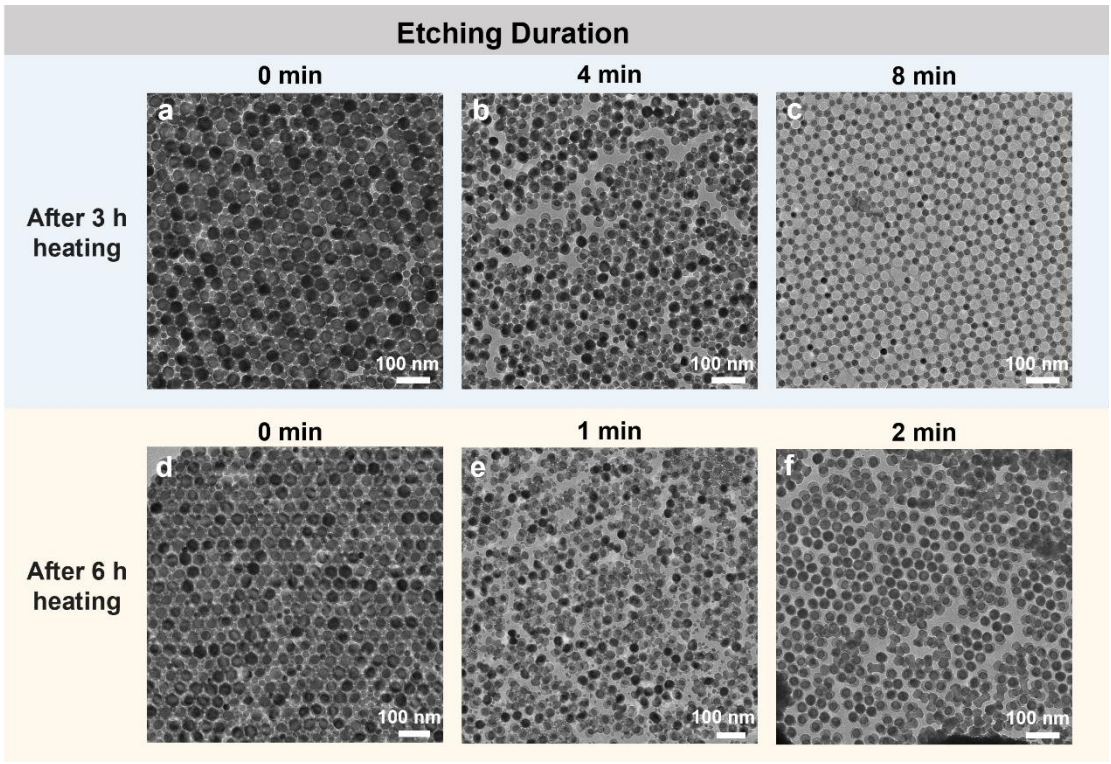

Figure S14. TEM images illustrating the duration-dependent, stepwise etching of AB_2-type nanodumbbells/sphere superlattices in oxalic acid. (a–c) Structures after thermal treatment at 150 °C for 3 h and etched in 0.05 M oxalic acid for 0, 4, and 8 min, showing selective removal of the nanodumbbells component while Fe_3O_4 spheres remain. (d–f) Structures after thermal treatment at 150 °C for 6 h and etched in 0.01 M oxalic acid for 0, 1, and 2 min, demonstrating preferential etching of Fe_3O_4 NCs with the NDs array preserved. The higher acid concentration required for nanodumbbells removal reflects the large volume mismatch between the two components.

Reference

1. D. Liu, X. Xu, Y. Du, X. Qin, Y. Zhang, C. Ma, S. Wen, W. Ren, E. M. Goldys, J. A. Piper, S. Dou, X. Liu and D. Jin, *Nat. Commun.*, 2016, **7**, 10254.

2. J. Park, K. An, Y. Hwang, J. G. Park, H. J. Noh, J. Y. Kim, J. H. Park, N. M. Hwang and T. Hyeon, *Nat. Mater.*, 2004, **3**, 891–895.

3. S. Y. Lee and M. T. Harris, *Journal of Colloid and Interface Science*, 2006, **293**, 401–408.

4. S. Wan, Y. Gao, Z. Zhang, F. Wu, Z. Zheng, H. Chen, X. Xi, D. Yang, T. Li, Z. Nie and A. Dong, *J. Am. Chem. Soc.*, 2024, **146**, 14225–14234.